Synthesis of *N*-(3-(4-[^{11}C]methylpiperazin-1-yl)-1-(5-methylpyridin-2-yl)-1*H*-pyrazol-5-yl)pyrazolo[1,5-*a*]pyrimidine-3-carboxamide as a new potential PET agent for imaging of IRAK4 enzyme in neuroinflammation

Xiaohong Wang[a], Wenzhi Xu[a], Caihong Miao[a], Fugui Dong[a], Wei Li[a], Min Wang[b], Mingzhang Gao[b], Qi-Huang Zheng[b,*], Zhidong Xu[a,*]

[a]*Key Laboratory of Medicinal Chemistry and Molecular Diagnosis of Ministry of Education, College of Chemistry and Environmental Science, Hebei University, Baoding, Hebei 071002, China*

[b]*Department of Radiology and Imaging Sciences, Indiana University School of Medicine, 1345 West 16th Street, Room 202, Indianapolis, IN 46202, USA*

***Corresponding authors:**

Qi-Huang Zheng, Ph.D.

Department of Radiology and Imaging Sciences

Indiana University School of Medicine

1345 West 16th Street, L3-202

Indianapolis, IN 46202

USA

E-mail: qzheng@iupui.edu

This is the author's manuscript of the article published in final edited form as:Wang, X., Xu, W., Miao, C., Dong, F., Li, W., Wang, M., … Xu, Z. (2017). Synthesis of N-(3-(4-[11C]methylpiperazin-1-yl)−1-(5-methylpyridin-2-yl)−1H-pyrazol-5-yl)pyrazolo[1,5-a]pyrimidine-3-carboxamide as a new potential PET agent for imaging of IRAK4 enzyme in neuroinflammation. Applied Radiation and Isotopes. https://doi.org/10.1016/j.apradiso.2017.11.005

Zhidong Xu, Ph.D.

Key Laboratory of Medicinal Chemistry and Molecular Diagnosis of Ministry of Education

College of Chemistry and Environmental Science

Hebei University, Baoding, Hebei 071002

China

E-mail: zhidongxu@hbu.edu.cn

Abstract

The reference standard *N*-(3-(4-methylpiperazin-1-yl)-1-(5-methylpyridin-2-yl)-1*H*-pyrazol-5-yl)pyrazolo[1,5-*a*]pyrimidine-3-carboxamide (**9**) and its demethylated precursor *N*-(1-(5-Methylpyridin-2-yl)-3-(piperazin-1-yl)-1*H*-pyrazol-5-yl)pyrazolo[1,5-*α*]pyrimidine-3-carboxamide (**8**) were synthesized from pyrazolo[1,5-*a*]pyrimidine-3-carboxylic acid and ethyl 2-cyanoacetate with overall chemical yield 13% in nine steps and 14% in eight steps, respectively. The target tracer *N*-(3-(4-[^{11}C]methylpiperazin-1-yl)-1-(5-methylpyridin-2-yl)-1*H*-pyrazol-5-yl)pyrazolo[1,5-*a*]pyrimidine-3-carboxamide ([^{11}C]**9**) was prepared from its precursor with [^{11}C]CH_3OTf through *N*-[^{11}C]methylation and isolated by HPLC combined with SPE in 50-60% radiochemical yield, based on [^{11}C]CO_2 and decay corrected to EOB. The radiochemical purity was >99%, and the specific activity at EOB was 370-1110 GBq/μmol.

Keywords: N-(3-(4-[^{11}C]methylpiperazin-1-yl)-1-(5-methylpyridin-2-yl)-1*H*-pyrazol-5-yl)pyrazolo[1,5-*a*]pyrimidine-3-carboxamide; Interleukin-1 receptor-associated kinase 4 (IRAK4); Radiosynthesis; Positron emission tomography (PET); Neuroinflammation

1. Introduction

Inflammation is a complex biological process and part of the body's immune response involving immune cells, blood vessels, and molecular mediators for self-protection to remove harmful stimuli, including damaged cells, irritants, or pathogens (Rodero and Crow, 2016). Neuroinflammation is the inflammation of the nervous tissue, and it is associated with central

nervous system (CNS) diseases like Alzheimer's disease (AD), Parkinson's disease (PD), Huntington's disease (HD), multiple sclerosis (MS), amyotrophic lateral sclerosis (ALS), traumatic brain injury (TBI) and stroke (Chen et al., 2016; Knzevic and Mizrahi, 2017; Rodero and Crow, 2016; Tronel et al., 2017). Molecular imaging of neuroinflammation in neurodegenerative diseases by positron emission tomography (PET) is one of the most active as well as most challenging areas in neuroscience, because PET neuroimaging can offer various non- or minimally invasive techniques to characterize neuroinflammatory processes for the purpose of diagnosis, therapy and treatment monitoring (Calsolaro and Edison, 2016; Cerami et al., 2017; Kielian, 2014; Schain and Kreisl, 2017). Many enzyme- or receptor-based radioligands have been developed for in vivo PET visualization of neuroinflammation (Albrecht et al., 2016; Gargiulo et al., 2017; Ory et al., 2014). We are interested in the development of new PET radioligands for neuroinflammation. In our previous work, we have synthesized and developed a series of PET radiotracers (Gao et al., 2010, 2011, 2015, 2017a; Territo et al., 2017; Wang et al., 2009; Zheng et al., 2003) that target the enzyme or receptor linked to neuroinflammation such as [^{11}C]FMAME for matrix metalloproteinase (MMP), carbon-11-labeled celecoxib derivatives for cyclooxygenase-2 (COX-2), [^{11}C]PBR28 for translocator protein (TSPO), [^{11}C]MCFA for cannabinoid receptor 2 (CB2), [^{11}C]GSK1482160 for purinergic receptor ($P2X_7$), and [^{11}C]methyl (2-amino-5-(benzylthio)thiazolo[4,5-*d*]pyrimidin-7-yl)-*D*-leucinate for CX_3C chemokine receptor 1 (CX_3CR1), as indicated in Figure 1. These PET tracers may have different imaging mechanisms, unfortunately, they have been found to have some drawbacks as an "inflammation" radiotracer. For example, in humans TSPO ligand [^{11}C]PBR28 exhibited high inter-subject variability in binding affinity, with a genetic polymorphism of the TSPO target resulting in population stratification into high-, mixed- and low-affinity binders (Yoder et al.,

2013). Thus, new "inflammation" PET tracers remain to be developed. In this ongoing study, we first select the enzyme interleukin-1 receptor-associated kinase 4 (IRAK4) as another more specific neuroinflammatory target for PET imaging. The enzyme IRAK4 represents a novel inflammation-associated molecular target. Radiotracers that target IRAK4 have the potential to overcome the limitations associated with previous "inflammation" radiotracers. IRAK4 is a critical upstream kinase in neuroinflammation and plays an important role in the progression of various neurodegenerative diseases (Jeong et al., 2017; Lv et al., 2017; Wang et al., 2014; Yuan et al., 2015). Recently, a potent and selective amidopyrazole inhibitor of IRAK4 with IC_{50} 5 nM, *N*-(3-(4-methylpiperazin-1-yl)-1-(5-methylpyridin-2-yl)-1*H*-pyrazol-5-yl)pyrazolo[1,5-*a*]pyrimidine-3-carboxamide (**9**), has been developed by Merck (McElroy et al., 2015). However, the PubMed search showed no records on radiolabeled IRAK4 inhibitors. Here we report the design and synthesis of a new carbon-11-labeled IRAK4 amidopyrazole inhibitor *N*-(3-(4-[^{11}C]methylpiperazin-1-yl)-1-(5-methylpyridin-2-yl)-1*H*-pyrazol-5-yl)pyrazolo[1,5-*a*]pyrimidine-3-carboxamide ([^{11}C]**9**) as a candidate PET neuroinflammation imaging agent.

Insert Figure 1 about here

2. Results and discussion

2.1. Chemistry

The reference standard **9** and its demethylated precursor *N*-(1-(5-methylpyridin-2-yl)-3-(piperazin-1-yl)-1*H*-pyrazol-5-yl)pyrazolo[1,5-*a*]pyrimidine-3-carboxamide (**8**) were synthesized as depicted in Scheme 1, according to the published procedures (Gopalsamy et al., 2009; Lim and Altman, 2015; McElroy et al., 2015) with modifications. Pyrazolo[1,5-*a*] pyrimidine-3-carbonyl chloride (**1**) was achieved by the reaction of commercially available pyrazolo[1,5-*a*]pyrimidine-3-carboxylic acid with thionly chloride. Compound **1** was used directly without further purification. 2-Cyano-3,3-bis(methylthio)acrylic acid (**3**) was prepared from ethyl 2-cyanoacetate by condensation with carbon disulfide in the presence of aqueous NaOH in EtOH, followed by hydrolysis with aqueous NaOH and methylation with dimethyl sulfate based on the reported procedure (Henriksen, 1996), with an overall chemical yield 54% for two steps. Commercially available *tert*-butyl piperazine-1-carboxylate and compound **3** underwent combined substitution and decarboxylation in the presence of trimethylamine (TEA) in MeOH to give (Z)-*tert*-butyl 4-(2-cyano-1-(methylthio)vinyl)piperazine-1-carboxylate (**4**) in 70% yield**.** Condensation of **4** with hydrazine monohydrate in EtOH afforded pyrazole derivative *tert*-butyl 4-(5-amino-1*H*-pyrazol-3-yl)piperazine-1-carboxylate (**5**) in 90% yield**.** Coupling of pyrazole derivative **5** and 2-bromo-5-methylpyridine employed CuI as catalyst, (1*S*,2*S*)-N^1,N^2-dimethylcyclohexane-1,2-diamine as organic ligand in the presence of Cs_2CO_3 in dimethyl sulfoxide (DMSO) to afforded *tert*-Butyl 4-(5-amino-1-(5-methylpyridin-2-yl)-1*H*-pyrazol-3-yl)piperazine-1-carboxylate (**6**) in 60% yield. Amidation of acyl halide **1** with amine **6** in the presence of *N*, *N*-diisopropylethylamine (DIPEA) in CH_2Cl_2 gave amide derivative **7** in 73% yield, which was deprotected Boc group with trifluoroacetic acid (TFA) in CH_2Cl_2 to yield the precursor **8** in 95% yield. *N*-methylation was performed by reductive amination of compound **8** with formaldehyde by $NaBH(OAC)_3$ in CH_2Cl_2 to obtain the reference standard **9** in 98% yield.

The specific modifications to the published synthetic procedures were major in the optimization of the reaction conditions in each step to improve the synthetic yield. For instance, we used TFA/CH_2Cl_2 instead of HCl/dioxane in the reported procedure (McElroy et al., 2015) for the deprotecting reaction of Boc group of compound **7** to give the precursor **8** in high yield.

Insert Scheme 1 about here

2.2. Radiochemistry

Synthesis of the target tracer ([^{11}C]**9**) is shown in Scheme 2. Demethylated precursor **8** underwent *N*-[^{11}C]methylation (Wang et al., 2013, 2015) using the reactive [^{11}C]methylating agent [^{11}C]methyl triflate ([^{11}C]CH_3OTf) (Jewett, 1992; Mock et al., 1999) in acetonitrile at 80 °C under basic conditions (2 N NaOH). The product was isolated by semi-preparative reverse-phase (RP) high performance liquid chromatography (HPLC) with a C-18 column, and then concentrated by solid-phase extraction (SPE) (Wang et al., 2011, 2012a) with a disposable C-18 Light Sep-Pak cartridge to produce the corresponding pure radiolabeled compound [^{11}C]**9** in 50-60% radiochemical yield, decay corrected to end of bombardment (EOB), based on [^{11}C]CO_2.

Insert Scheme 2 about here

The radiosynthesis included three stages: 1) labeling reaction; 2) purification; and 3) formulation. We employed more reactive [^{11}C]CH_3OTf, instead of commonly used [^{11}C]methyl iodide ([^{11}C]CH_3I) (Allard et al., 2008), in *N*-[^{11}C]methylation to improve radiochemical yield of

[^{11}C]**9**. We used an Eckert & Ziegler Modular Lab C-11 Methyl Iodide/Triflate module to produce [^{11}C]methylating agent either [^{11}C]CH_3OTf or [^{11}C]CH_3I ([^{11}C]CH_3Br passed through a NaI column). The direct comparison between [^{11}C]CH_3OTf and [^{11}C]CH_3I confirmed the result. The labeling reaction was conducted using a V-vial method. Addition of aqueous $NaHCO_3$ to quench the radiolabeling reaction and to dilute the radiolabeling mixture prior to the injection onto the semi-preparative HPLC column for purification gave better separation of [^{11}C]**9** from its 3-(piperazin-1-yl) precursor **8**. We used Sep-Pak trap/release method instead of rotatory evaporation for formulation to improve the chemical purity of radiolabeled product [^{11}C]**9**. In addition, a C18 Light Sep-Pak to replace a C18 Plus Sep-Pak allowed final product formulation with ≤5% ethanol (Zheng et al., 2015). Overall, it took ~40 min for synthesis, purification and dose formulation.

The radiosynthesis was performed in a home-built automated multi-purpose [^{11}C]-radiosynthesis module (Mock et al., 2005a,b; Wang et al, 2012b). This radiosynthesis module facilitated the overall design of the reaction, purification and reformulation capabilities in a fashion suitable for adaptation to preparation of human doses. In addition, the module is designed to allow in-process measurement of [^{11}C]-tracer specific activity (SA, GBq/μmol at EOB) using a radiation detector at the outlet of the HPLC-portion of the system. For the reported syntheses, product SA was in a range of 370-1110 GBq/μmol at EOB. The major factors including [^{11}C]-target and [^{11}C]-radiosynthesis unit that affect the EOB SA significantly to lead to such a wide range from 370 to 1110 GBq/μmol have been discussed in our previous works (Gao et al., 2016a). The general methods to increase SA have been described as well, and the SA of our [^{11}C]-tracers is significantly improved (Glick-Wilson et al., 2017). The 'wide range' of SA we reported is for the

same [^{11}C]-tracer produced in different days, because very different [^{11}C]-target and [^{11}C]-radiosynthesis unit situations would make SA in a wide range. For a [^{11}C]-tracer produced in the same day, the SA of the same tracer in different production runs will be in a small range, because [^{11}C]-target and [^{11}C]-radiosynthesis unit would not be much different in the same day. Likewise, the methods to minimize such wide range of SA from practice perspective have been provided in our previous works (Gao et al., 2017b). At the end of synthesis (EOS), the SA of [^{11}C]-tracer was determined again by analytical HPLC (Zheng and Mock, 2005), calculated, decay corrected to EOB, and based on [^{11}C]CO_2, which was in agreement with the 'on line' determined value. In each our [^{11}C]-tracer production, if semi-preparative HPLC was used for purification, then the SA of [^{11}C]-tracer was assessed by both semi-preparative HPLC (during synthesis) and analytical HPLC (EOS); if SPE was used for purification, then the SA of [^{11}C]-tracer was only measured by analytical HPLC at EOS (Gao et al., 2016b).

Chemical purity and radiochemical purity were determined by analytical HPLC (Zheng and Mock, 2005). The chemical purity of the precursor and reference standard was >99%. The radiochemical purity of the target tracer was >99% determined by radio-HPLC through γ-ray (PIN diode) flow detector, and the chemical purity of the target tracer was >85% determined by reversed-phase HPLC through UV flow detector.

3. Experimental

3.1. General

All commercial reagents and solvents were purchased from Sigma-Aldrich and Fisher Scientific, and used without further purification. [^{11}C]CH_3OTf was prepared according to a literature procedure (Mock et al., 1999). Melting points were determined on WRR apparatus and were uncorrected. ^{1}H NMR spectra were recorded on a Bruker Avance II 600 MHz NMR Fourier transform spectrometer. Chemical shifts (δ) are reported in parts per million (ppm) relative to an internal standard tetramethylsilane (TMS, δ 0.0), and coupling constants (J) are reported in hertz (Hz). Liquid chromatography-mass spectra (LC-MS) analysis was performed on AB Sciex 4000Q Trap instrument, consisting of an 1100 series HPLC connected to a diode array detector and a 1946D mass spectrometer configured for positive-ion/negative-ion electrospray ionization (ESI). The high resolution mass spectra (HRMS) were obtained using a Waters/Micromass LCT Classic spectrometer. Chromatographic solvent proportions are indicated as volume: volume ratio. Thin-layer chromatography (TLC) was run using HS silica gel GF254 uniplates (5 × 10 cm^2). Plates were visualized under UV light. Preparative TLC was run using HS silica gel UV254 plates (20 × 20 cm^2). Normal phase flash column chromatography was carried out on Combiflash Rf 150 silica gel 60 (300-400 mesh) with a forced flow of the indicated solvent system in the proportions described below. All moisture- and air-sensitive reactions were performed under a positive pressure of nitrogen maintained by a direct line from a nitrogen source. Analytical RP HPLC was performed using a Prodigy (Phenomenex) 5 μm C-18 column, 4.6 × 250 mm; mobile phase 30%CH_3CN/70% 0.05% TFA; flow rate 1.0 mL/min; UV (254 nm) and γ-ray (PIN diode) flow detectors. Semi-preparative RP HPLC was performed using a Prodigy (Phenomenex) 5 μm C-18 column, 10 × 250 mm; mobile phase 30%CH_3CN/70% 20 mM H_3PO_4; flow rate 4 mL/min; UV (254 nm) and γ-ray (PIN diode) flow detectors. C18 Light

Sep-Pak cartridges were obtained from Waters Corporation (Milford, MA). Sterile Millex-FG 0.2 μm filter units were obtained from Millipore Corporation (Bedford, MA).

*3.2. Pyrazolo[1,5-a]pyrimidine-3-carbonyl chloride (**1**)*

A solution of pyrazolo[1,5-*a*]pyrimidine-3-carboxylic acid (102 mg, 0.62 mmol) in thionyl chloride (10.0 g, 6.2 mL, 84 mmol) was stirred and heated at reflux for 1.5 h. Excess thionyl chloride was removed *in vacuo*, the crude product was washed with hexanes and dried *in vacuo* to afford compound **1** as a yellow solid (112 mg, 100%), which was used directly for preparing compound **7**.

*3.3. Sodium 2-cyano-3-ethoxy-3-oxoprop-1-ene-1,1-bis(thiolate) (**2**)*

A stirred mixture of ethyl 2-cyanoacetate (16.0 g, 141.5 mmol) and carbon disulfide (10.7 g, 141.7 mmol) in EtOH (50 mL) was cooled to 0 °C, followed by addition of a solution of NaOH (11.3 g, 283 mmol) in water (11.3 mL) dropwise at 0 °C. Then the reaction mixture was warmed to room temperature (RT) and stirred for 30 min. The precipitation was filtered, washed with anhydrous ethanol and dried *in vacuo* to afford compound **2** as a yellow solid (29.9 g, 90%), mp 90.0-91.5 °C. ^{1}H NMR (D_2O): δ 4.08 (q, J = 7.1 Hz, 2H), 1.20 (t, J = 7.1 Hz, 3H).

*3.4. 2-Cyano-3,3-bis(methylthio)acrylic acid (**3**)*

A mixture of compound **2** (29.9 g, 128.3 mmol) and NaOH (8.7 g, 218 mmol) in water (60 mL) was stirred and heated at 40 °C for 6 h. After the reaction mixture was cooled to 0 °C, anhydrous ethanol (100 mL) was added dropwise at 0 °C. The aqueous layer was separated and diluted with water (100 mL), followed by addition of dimethyl sulfate (27.5 g, 18.7 mmol) at 0 °C. After the mixture was warmed to RT and stirred for 30 min, it was cooled to 0 °C and filtered. The filtrate was adjusted with 6 M HCl to pH 2, the precipitate was filtered and dried *in vacuo* to afford **3** as a white solid (14.5 g, 60%), mp 107.3-108.5 °C. ^{1}H NMR (DMSO-d_6): δ 2.69 (s, 3H), 2.58 (s, 3H).

*3.5. tert-Butyl (Z)-4-(2-cyano-1-(methylthio)vinyl)piperazine-1-carboxylate (**4**)*

To a stirred solution of compound **3** (706 mg, 3.7 mmol) in MeOH (30 mL), trimethylamine (318.0 mg, 3.7 mmol) was added at 0 °C, followed by addition of *tert*-butyl piperazine-1-carboxylate (1.4 g, 7.7 mmol). After the reaction mixture was stirred at 0 °C for 12 h, it was diluted with water and extracted with EtOAc. The combined organic layer was washed with brine, dried over anhydrous Na_2SO_4 and filtered. The solvent was evaporated *in vacuo*. The crude product was purified by silica gel column chromatography with petroleum ether (PE)/EtOAc (9:1 to 7:3) as eluent to afford **4** as a white solid (735 mg, 70%), mp 51.1-53.5 °C. ^{1}H NMR (DMSO-d_6): δ 4.61 (s, 1H), 3.37 (t, J = 5.2 Hz, 4H), 3.30 (t, J = 5.2 Hz, 4H), 2.34 (s, 3H), 1.42 (s, 9H). LC-MS (ESI, *m/z*): Calcd for $C_{13}H_{21}N_3O_2SNa$ ($[M+Na]^+$) 306.1, found: 306.0.

*3.6. tert-Butyl 4-(5-amino-1H-pyrazol-3-yl)piperazine-1-carboxylate (**5**)*

A mixture of compound **4** (590 mg, 2.08 mmol) and hydrazine monohydrate (250 mg, 5.0 mmol) in EtOH (5 mL) was stirred and heated at reflux for 14 h. After the reaction mixture was cooled to RT, it was diluted with water and extracted with CH_2Cl_2. The combined organic layer was washed with brine, dried over anhydrous Na_2SO_4 and filtered. The organic solvent was evaporated *in vacuo*. The crude product was purified by silica gel column chromatography with CH_2Cl_2/MeOH (100:1 to 9:1) as eluent to afford **5** as a white solid (510 mg, 90%), mp 133.5-135.8 °C. ^{1}H NMR ($CDCl_3$): δ 5.30 (s, 1H), 4.99 (s, 1H), 3.50 (t, J = 4.3 Hz, 4H), 3.06 (t, J = 4.3 Hz, 4H), 1.46 (s, 9H). LC-MS (ESI, *m/z*): Calcd for $C_{12}H_{21}N_5O_2Na$ ($[M+Na]^+$) 290.2, found: 290.2.

*3.7. tert-Butyl 4-(5-amino-1-(5-methylpyridin-2-yl)-1H-pyrazol-3-yl)piperazine-1-carboxylate (**6**)*

A mixture of compound **5** (300 mg, 1.1 mmol), 2-bromo-5-methylpyridine (234 mg, 1.2 mmol), CuI (22 mg, 0.1 mmol), (1*S*,2*S*)-N^1,N^2-dimethylcyclohexane-1,2-diamine (16 mg, 0.1 mmol) and Cs_2CO_3 (734 mg, 2.3 mmol) in DMSO (3 mL) was purged with N_2 for 10 min. The reaction mixture was heated at 130 °C in a sealed tube for 15 h. After the reaction mixture was cooled to RT, it was diluted with water (30 mL) and extracted with EtOAc. The combined organic layer was washed with brine, dried over anhydrous Na_2SO_4 and filtered. The organic solvent was evaporated *in vacuo*. The crude product was purified by silica gel column chromatography with PE/EtOAc (100:1 to 3:2) as eluent to afford **6** as a white solid (336 mg, 60%), mp 145.6-152.0 °C. ^{1}H NMR ($CDCl_3$): δ 8.06 (s, 1H), 7.69 (d, J = 8.6 Hz, 1H), 7.52 (d, J = 8.6 Hz, 1H), 5.92 (s,

2H), 5.04 (s, 1H), 3.53 (t, *J* = 5.0 Hz, 4H), 3.21 (t, *J* = 5.0 Hz, 4H), 2.29 (s, 3H), 1.47 (s, 9H). HRMS (ESI, *m/z*): Calcd for $C_{18}H_{26}N_6O_2$ ($[M+H]^+$) 359.2190, found: 359.2188.

*3.8. tert-Butyl 4-(1-(5-methylpyridin-2-yl)-5-(pyrazolo[1,5-a]pyrimidine-3-carboxamido)-1H-pyrazol-3-yl)piperazine-1-carboxylate (**7**)*

To a stirred solution of compound **1** (112 mg, 0.62 mmol) in CH_2Cl_2 (5 mL) was added compound **6** (92 mg, 0.33 mmol) and DIPEA (60 μL). After the reaction mixture was stirred at RT for 2 h, it was diluted with water and extracted with CH_2Cl_2. The combined organic layer was washed with brine, dried over anhydrous Na_2SO_4 and filtered. The organic solvent was evaporated *in vacuo*. The crude product was purified by silica gel column chromatography with PE/EtOAc (100:1 to 1:1) to afford **7** as a white solid (121 mg, 73%), mp 187.4-188.2 °C. ^{1}H NMR ($CDCl_3$): δ 13.36 (s, 1H), 8.85 (dd, *J* = 4.1, 1.7 Hz, 1H), 8.84-8.83 (dd, *J* = 7.0, 1.7 Hz, 1H), 8.78 (s, 1H), 8.24 (s, 1H), 7.79 (d, *J* = 8.5 Hz, 1H), 7.61 (dd, *J* = 8.5, 2.0 Hz), 7.09 (dd, *J* = 7.0, 4.1 Hz, 1H), 6.76 (s, 1H), 3.57 (s, 4H), 3.33 (s, 4H), 2.37 (s, 3H), 1.49 (s, 9H). LC-MS (ESI, *m/z*): Calcd for $C_{25}H_{29}N_9O_3Na$ ($[M+Na]^+$) 526.1, found: 526.1.

*3.9. N-(1-(5-Methylpyridin-2-yl)-3-(piperazin-1-yl)-1H-pyrazol-5-yl)pyrazolo[1,5-α]pyrimidine-3-carboxamide (**8**)*

To a stirred solution of compound **7** (219 mg, 0.44 mmol) in CH_2Cl_2 (10 mL) was added TFA (1 mL) dropwise. After the reaction mixture was stirred at RT for 2 h, the solvent was removed *in vavuo*. The residual was diluted with water, adjusted with 3 N NaOH to pH 10 and extracted

with CH_2Cl_2. The combined organic layer was washed with brine, dried over anhydrous Na_2SO_4 and filtered. The organic solvent was evaporated *in vacuo*. The crude product was purified by silica gel column chromatography with CH_2Cl_2/MeOH (100:1 to 9:1) to afford **8** as a white solid (167 mg, 95%), mp 209.9-211.3 °C. ^{1}H NMR ($CDCl_3$): δ 13.32 (s, 1H), 8.82 (dd, J = 4.1, 1.7 Hz, 1H), 8.81 (dd, J = 6.9, 1.7 Hz, 1H), 8.76 (s, 1H), 8.22 (s, 1H),7.77 (d, J = 8.5 Hz, 1H), 7.59 (dd, J = 8.5, 2.0 Hz, 1H), 7.06 (dd, J = 6.9, 4.1 Hz, 1H), 6.75 (s, 1H), 3.34 (t, J = 4.8 Hz, 4H), 3.03 (t, J = 4.8 Hz, 4H),2.36 (s, 3H). LC-MS (ESI, *m/z*): Calcd for $C_{20}H_{21}N_9O$ ($[M+H]^+$) 404.1, found: 404.2. HRMS (ESI, *m/z*): Calcd for $C_{20}H_{21}N_9O$ ($[M+H]^+$) 404.1941, found: 404.1937.

*3.10. N-(3-(4-methylpiperazin-1-yl)-1-(5-methylpyridin-2-yl)-1H-pyrazol-5-yl)pyrazolo[1,5-a]pyrimidine-3-carboxamide (**9**)*

To a stirred solution of compound **8** (167 mg, 0.41mmol) in CH_2Cl_2 (10 mL) was added formaldehyde (100 μL, 37% solution in water, 1.23 mmol) and DIPEA (170 μL, 1.23 mmol). After the reaction mixture was stirred at RT for 20 min, $NaBH(OAc)_3$ (318 mg, 1.5 mmol) was added and the mixture was stirred at RT for 20 h. The reaction was quenched with saturated $NaHCO_3$ (30 mL) and extracted with CH_2Cl_2. The combined organic layer was washed with brine, dried over anhydrous Na_2SO_4 and filtered. The organic solvent was evaporated *in vacuo*. The crude product was purified by silica gel column chromatography with CH_2Cl_2/MeOH (100:1 to 9:1) to afford **9** as a white solid (167 mg, 98%), mp 218.3-219.9 °C. ^{1}H NMR ($CDCl_3$): δ 13.34 (s, 1H), 8.84 (dd, J = 4.0, 1.5 Hz, 1H), 8.83 (dd, J = 6.9, 1.5 Hz, 1H), 8.78 (s, 1H), 8.24 (s, 1H), 7.79 (d, J = 8.5 Hz, 1H), 7.59 (dd, J = 8.5, 1.9Hz, 1H), 7.08 (dd, J = 6.9, 4.0 Hz, 1H), 6.76 (s, 1H), 3.42 (t, J = 4.5 Hz, 4H), 2.58 (t, J = 4.5 Hz, 4H), 2.36 (s, 3H), 2.17 (s, 3H). LC-MS (ESI,

m/z): Calcd for $C_{21}H_{23}N_9O$ ([M+H]$^+$) 418.2, found: 418.2. HRMS (ESI, *m/z*): Calcd for $C_{21}H_{23}N_9O$ ([M+H]$^+$) 418.2098, found: 418.2093.

*3.11. N-(3-(4-[^{11}C]methylpiperazin-1-yl)-1-(5-methylpyridin-2-yl)-1H-pyrazol-5-yl)pyrazolo[1,5-a]pyrimidine-3-carboxamide ([^{11}C]**9**)*

[^{11}C]CO_2 was produced by the $^{14}N(p,\alpha)^{11}C$ nuclear reaction in the small volume (9.5 cm^3) aluminum gas target provided with the Siemens RDS-111 Eclipse cyclotron. The target gas consisted of 1% oxygen in nitrogen purchased as a specialty gas from Praxair, Indianapolis, IN. Typical irradiations used for the development were 58 μA beam current and 15 min on target. The production run produced approximately 25.9 GBq of [^{11}C]CO_2 at EOB. Demethylated precursor **8** (0.1-0.3 mg) was dissolved in CH_3CN (300 μL). To this solution was added aqueous NaOH (2 N, 2 μL). The mixture was transferred to a small reaction vial. No-carrier-added (high specific activity) [^{11}C]CH_3OTf that was produced by the gas-phase production method (Mock et al., 1999) within 12 min from [^{11}C]CO_2 through [^{11}C]CH_4 and [^{11}C]CH_3Br with silver triflate (AgOTf) column was passed into the reaction vial at RT until radioactivity reached a maximum (2 min), and then the reaction vial was isolated and heated at 80 °C for 3 min. The contents of the reaction vial were diluted with aqueous $NaHCO_3$ (0.1 M, 1 mL). The reaction vial was connected to a 3-mL HPLC injection loop. The labeled product mixture solution was injected onto the semi-preparative HPLC column for purification. The product fraction was collected in a recovery vial containing 30 mL water. The diluted tracer solution was then passed through a C-18 Sep-Pak Light cartridge, and washed with water (3 × 10 mL). The cartridge was eluted with EtOH (3 × 0.4 mL) to release the labeled product, followed by saline (10-11 mL). The eluted product was

then sterile-filtered through a Millex-FG 0.2 μm membrane into a sterile vial. Total radioactivity was assayed and total volume (10-11 mL) was noted for tracer dose dispensing. The overall synthesis time including HPLC-SPE purification and reformulation was ~40 min from EOB. The decay corrected radiochemical yield was 50-60%. Retention times in the analytical HPLC system were: t_R **8** = 6.86 min, t_R **9** = 7.66 min, t_R [^{11}C]**9** = 7.82 min. Retention times in the preparative HPLC system were: t_R **8** = 5.85 min, t_R **9** = 8.53 min, t_R [^{11}C]**9** = 8.87 min.

4. Conclusion

In summary, synthetic routes with moderate to high yields have been developed to produce the reference standard **9**, demethylated precursor **8** and target tracer [^{11}C]**9**. The radiosynthesis employed [^{11}C]CH_3OTf for *N*-[^{11}C]methylation at the piperazin position of the desmethyl precursor, followed by product purification and isolation using a semi-preparative RP HPLC combined with SPE. [^{11}C]**9** was obtained in high radiochemical yield, radiochemical purity and chemical purity, with a reasonably short overall synthesis time, and high specific activity. This will facilitate studies to evaluate [^{11}C]**9** as a new potential PET agent for imaging of IRAK4 enzyme in neuroinflammation.

Conflict of interest statement

The authors declare that they have no conflict of interest relevant to this article.

Acknowledgments

This work was partially supported by the Hebei Province Major Science and Technology Program (No. 17392605D) and the Hundred-Talent Program of Hebei Province (No. E2015100012), China. This work was also partially supported by the Advanced Imaging Research and Technology Development (AIRTD) grants from the Indiana University Department of Radiology and Imaging Sciences in the United States.

References

Albrecht, D.S., Granziera, C., Hooker, J.M., Loggia, M.L., 2016. In vivo imaging of human neuroinflammation. ACS Chem. Neurosci. 7, 470-483.

Allard, M., Fouquet, E., James, D., Szlosek-Pinaud, M., 2008. State of art in ^{11}C labelled radiotracers synthesis. Curr. Med. Chem. 15, 235-277.

Calsolaro, V., Edison, P., 2016. Neuroinflammation in Alzheimer's disease: Current evidence and future directions. Alzheimer's Dement. 12, 719-732.

Cerami, C., Iaccarino, L., Perani, D., 2017. Molecular imaging of neuroinflammation in neurodegenerative dementias: The role of in vivo PET imaging. Int. J. Mol. Sci. 18, E993.

Chen, W.-W., Zhang, X., Huang, W.-J., 2016. Role of neuroinflammation in neurodegenerative diseases (review). Mol. Med. Rep. 13, 3391-3396.

Gao, M., Wang, M., Miller, K.D., Hutchins, G.D., Zheng, Q.-H., 2010. Synthesis and in vitro biological evaluation of carbon-11-labeled quinoline derivatives as new candidate PET radioligands for cannabinoid CB2 receptor imaging. Bioorg. Med. Chem. 18, 2099-2106.

Gao, M., Wang, M., Miller, K.D., Zheng, Q.-H., 2011. Synthesis and preliminary in vitro biological evaluation of new carbon-11-labeled celecoxib derivatives as candidate PET tracers for imaging of COX-2 expression in cancer. Eur. J. Med. Chem. 46, 4760-4767.

Gao, M., Wang, M., Green, M.A., Hutchins, G.D., Zheng, Q.-H., 2015. Synthesis of [^{11}C]GSK1482160 as a new PET agent for targeting $P2X_7$ receptor. Bioorg. Med. Chem. Lett. 25, 1965-1970.

Gao, M., Wang, M., Zheng, Q.-H., 2016a. Synthesis of carbon-11-labeled imidazopyridine- and purine-thioacetamide derivatives as new potential PET tracers for imaging of nucleotide pyrophosphatase/phosphodiesterase 1 (NPP1). Bioorg. Med. Chem. Lett. 26, 1371-1375.

Gao, M., Wang, M., Zheng, Q.-H., 2016b. Synthesis of [^{11}C]MK-1064 as a new PET radioligand for imaging of orexin-2 receptor. Bioorg. Med. Chem. Lett. 26, 3694-3699.

Gao, M., Wang, M., Meyers, J.A., Peters, J.S., Zarrinmayeh, H., Territo, P.R., Hutchins, G.D., Zheng, Q.-H., 2017a. Synthesis and preliminary biological evaluation of [^{11}C]methyl (2-amino-5-(benzylthio)thiazolo[4,5-*d*]pyrimidin-7-yl)-*D*-leucinate for the fractalkine receptor (CX_3CR1). Bioorg. Med. Chem. Lett. 27, 2727-2730.

Gao, M., Wang, M., Zheng, Q.-H., 2017b. Synthesis of carbon-11-labeled isonicotinamides as new potential PET agents for imaging of GSK-3 enzyme in Alzheimer's disease. Bioorg. Med. Chem. Lett. 27, 740-743.

Gargiulo, S., Coda, A.R., Panico, M., Gramanzini, M., Moresco, R.M., Chalon, S., Pappata, S., 2017. Molecular imaging of neuroinflammation in preclinical rodent models using positron emission tomography. Q. J. Nucl. Med. Mol. Imaging 61, 60-75.

Glick-Wilson, B.E., Wang, M., Corbin, L.A., Gao, M., Wissmann, C.L., Zheng, Q.-H., 2017. General method to increase the specific activity of carbon-11-labeled compounds produced from [^{11}C]CH_3OTf. J. Label. Compd. Radiopharm. 60, S284.

Gopalsamy, A., Ciszewski, G., Shi, M., Berger, D., Hu, Y., Lee, F., Feldberg, L., Frommer, E., Kim, S., Collins, K., Wojciechowicz, D., Mallon, R., 2009. Hit to lead optimization of pyrazolo[1,5-α]pyrimidines as B-Raf kinase inhibitors. Bioorg. Med. Chem. Lett. 19, 6890-6892.

Henriksen, L., 1996. Sodium 2-cyanoethylene-1,1-dithiolate tetrahydrate: a stable salt of cyanodithioacetic acid. A new preparative route to 2-cyanoketene *S*,S-, *S*,*N*- and *N*,*N*-acetals. Acta Chem. Scand. 50, 432-437.

Jeong, Y.-H., Park, J.-S., Kim, D.-H., Kang, J.L., Kim, H.-S., 2017. Anti-inflammatory mechanism of lonchocarpine in LPS- or poly(I:C)-induced neuroinflammation. Pharmacol. Res. 119, 431-442.

Jewett, D.M., 1992. A simple synthesis of [^{11}C]methyl triflate. Int. J. Rad. Appl. Instrum. A 43, 1383-1385.

Kielian, T., 2014. Neuroinflammation: good, bad, or indifferent? J. Neurochem. 130, 1-3.

Knezevic, D., Mizrahi, R., 2018. Molecular imaging of neuroinflammation in Alzheimer's disease and mild cognitive impairment. Prog. Neuropsychopharmacol. Biol. Psychiatry 80, 123-131.

Lim, J., Altman, M.D., 2015. Substituted amidopyrazole inhibitors of Interleukin receptor-associated kinases (IRAK-4). WO 2015/006181 A1.

Lv, Y.-N., Qu-Yang, A.J., Fu, L.-S., 2017. MicroRNA-27a Negatively Modulates the Inflammatory Response in Lipopolysaccharide-Stimulated Microglia by Targeting TLR4 and IRAK4. Cell Mol. Neurobiol. 37, 195-210.

McElroy, W.T., Tan Z., Ho G., Paliwal, S., Li, G., Seganish, W.M., Tulshian, D., Tata, J., Fischmann, T.O., Sondey, C., Bian, H., Bober, L., Jackson, J., Garlisi, C.G., Devito, K., Fossetta, J., Lundell, D., Niu, X., 2015. Potent and selective amidopyrazole inhibitors of IRAK4 that are efficacious in a rodent model of inflammation. ACS Med. Chem. Lett. 6, 677-682.

Mock, B.H., Mulholland, G.K., Vavrek, M.T., 1999. Convenient gas phase bromination of [^{11}C]methane and production of [^{11}C]methyl triflate. Nucl. Med. Biol. 26, 467-471.

Mock, B.H., Glick-Wilson, B.E., Zheng, Q.-H., DeGrado, T.R., 2005a. Automated measurement of specific activity of radiolabeled ligands during synthesis. J. Label. Compd. Radiopharm. 48, S224.

Mock, B.H., Zheng, Q.-H., DeGrado, T.R., 2005b. A multi-purpose ^{11}C-radio-synthesis system. J. Label. Compd. Radiopharm. 48, S225.

Ory, D., Celen, S., Verbruggen, A., Bormans, G., 2014. PET radioligands for in vivo visualization of neuroinflammation. Curr. Pharm. Des. 20, 5897-5913.

Rodero, M.P., Crow, Y.J., 2016. Type I interferon-mediated monogenic autoinflammation: The type I interferonopathies, a conceptual overview. J. Exp. Med. 13, 2527-2538.

Schain, M., Kreisl, W.C., 2017. Neuroinflammation in Neurodegenerative Disorders-a Review. Curr. Neurol. Neurosci. Rep. 17, 25.

Territo, P.R., Meyer, J.A., Peters, J.S., Riley, A.A., McCarthy, B.P., Gao, M., Wang, M., Green, M.A., Zheng, Q.-H., Hutchins, G.D., 2017. Characterization of ^{11}C-GSK1482160 for targeting the P2X7 receptor as a biomarker for neuroinflammation. J. Nucl. Med. 58, 458-465.

Tronel, C., Largeau, B., Santiago Ribeiro, M.J., Guilloteau, D., Dupont, A.C., Arlicot, N., 2017. Molecular targets for PET imaging of activated microglia: The current situation and future expectations. Int. J. Mol. Sci. 18, E802.

Wang, M., Yoder, K.K., Gao, M., Mock, B.H., Xu, X.-M., Saykin, A.J., Hutchins, G.D., Zheng, Q.-H., 2009. Fully automated synthesis and initial PET imaging of [^{11}C]PBR28. Bioorg. Med. Chem. Lett. 19, 5636-5639.

Wang, M., Gao, M., Miller, K.D., Zheng, Q.-H., 2011. Synthesis of [^{11}C]PBR06 and [^{18}F]PBR06 as agents for positron emission tomographic (PET) imaging of the translocator protein (TSPO). Steroids 76, 1331-1340.

Wang, M., Gao, M., Miller, K.D., Sledge, G.W., Zheng, Q.-H., 2012a. [^{11}C]GSK2126458 and [^{18}F]GSK2126458, the first radiosynthesis of new potential PET agents for imaging of PI3K and mTOR in cancers. Bioorg. Med. Chem. Lett. 22, 1569-1574.

Wang, M., Gao, M., Zheng, Q.-H., 2012b. Fully automated synthesis of PET TSPO radioligands [^{11}C]DAA1106 and [^{18}F]FEDAA1106. Appl. Radiat. Isot. 70, 965-973.

Wang, M., Gao, M., Zheng, Q.-H., 2013. A high-yield route to synthesize the P-glycoprotein radioligand [^{11}C]*N*-desmethyl-loperamide and its parent radioligand [^{11}C]loperamide. Bioorg. Med. Chem. Lett. 23, 5259-5263.

Wang, M., Gao, M., Xu, Z., Zheng, Q.-H., 2015. Synthesis of a PET tau tracer [^{11}C]PBB3 for imaging of Alzheimer's disease. Bioorg. Med. Chem. Lett. 25, 4587-4592.

Wang, Y., Ge, P., Yang, L., Wu, C., Zha, H., Luo, T., Zhu, Y., 2014. Protection of ischemic post conditioning against transient focal ischemia-induced brain damage is associated with inhibition of neuroinflammation via modulation of TLR2 and TLR4 pathways. J. Neuroinflammation 11, 15.

Yoder, K.K., Nho, K., Risacher, S.L., Kim, S., Shen, L., Saykin, A.J., 2013. Influence of TSPO genotype in ^{11}C-PBR28 standardized uptake values. J. Nucl. Med. 54, 1320-1322.

Yuan, B., Shen, H., Lin, L., Su, T., Zhong, L., Yang, Z., 2015. MicroRNA367 negatively regulates the inflammatory response of microglia by targeting IRAK4 in intracerebral hemorrhage. J. Neuroinflammation 12, 206.

Zheng, Q.-H., Fei, X., DeGrado, T.R., Wang, J.-Q., Stone, K.L., Martinez, T.D., Gay, D.J., Baity, W.L., Mock, B.H., Glick-Wilson, B.E., Sullivan, M.L., Miller, K.D., Sledge, G.W., Hutchins, G.D., 2003. Synthesis, biodistribution and micro-PET imaging of a potential cancer biomarker carbon-11 labeled MMP inhibitor (2R)-2-[[4-(6-fluorohex-1-ynyl)phenyl]sulfonylamino]-3-methylbutyric acid [^{11}C]methyl ester. Nucl. Med. Biol. 30, 753-760.

Zheng, Q.-H., Mock, B.H., 2005. Purification of carbon-11 PET radiotracers from unlabeled precursors by preparative HPLC and SPE. Biomed. Chromatogr. 19, 671-676.

Zheng, Q.-H., Glick-Wilson, B.E., Steele, B.L., Shaffer, M., Corbin, L.A., Green, M.A., 2015. A simplified conventional manual C18 Light Sep-Pak system for purification and reformulation of carbon-11 PET tracers. J. Label. Compd. Radiopharm. 58, S392.

Figure and Scheme Legends

Figure 1. PET radiotracers for imaging of neuroinflammation.

Scheme 1. Synthesis of *N*-(3-(4-methylpiperazin-1-yl)-1-(5-methylpyridin-2-yl)-1*H*-pyrazol-5-yl)pyrazolo[1,5-*a*]pyrimidine-3-carboxamide (**9**) and *N*-(1-(5-Methylpyridin-2-yl)-3-(piperazin-1-yl)-1*H*-pyrazol-5-yl)pyrazolo[1,5-*α*]pyrimidine-3-carboxamide (**8**).

Scheme 2. Synthesis of *N*-(3-(4-[^{11}C]methylpiperazin-1-yl)-1-(5-methylpyridin-2-yl)-1*H*-pyrazol-5-yl)pyrazolo[1,5-*a*]pyrimidine-3-carboxamide ([^{11}C]**9**).

Figure 1.

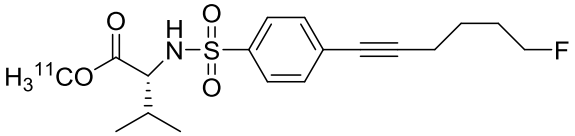

[^{11}C]FMAME (MMP)

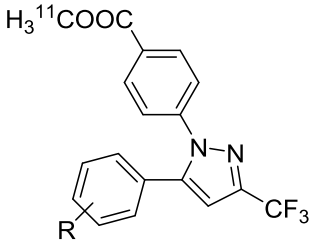

Carbon-11-labeled celecoxib derivatives (COX-2)
R=2-OMe; 3-OMe; 4-OMe; 4-Me

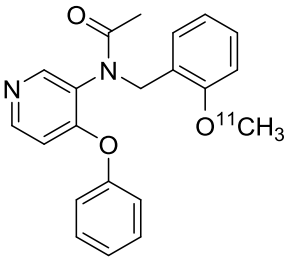

[^{11}C]PBR28 (TSPO)

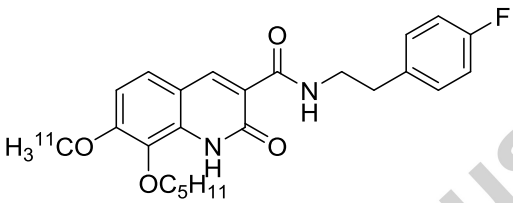

[^{11}C]MCFA (CB2)

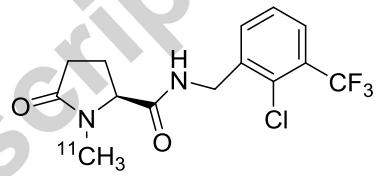

[^{11}C]GSK1482160 (P2X$_7$)

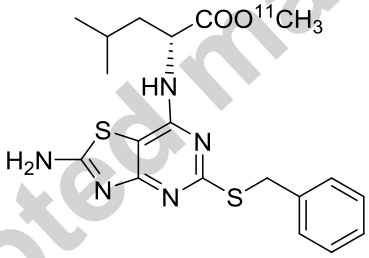

[^{11}C]Methyl (2-amino-5-(benzylthio)thiazolo[4,5-*d*]pyrimidin-7-yl)-*D*-leucinate (CX$_3$CR1)

Scheme 1.

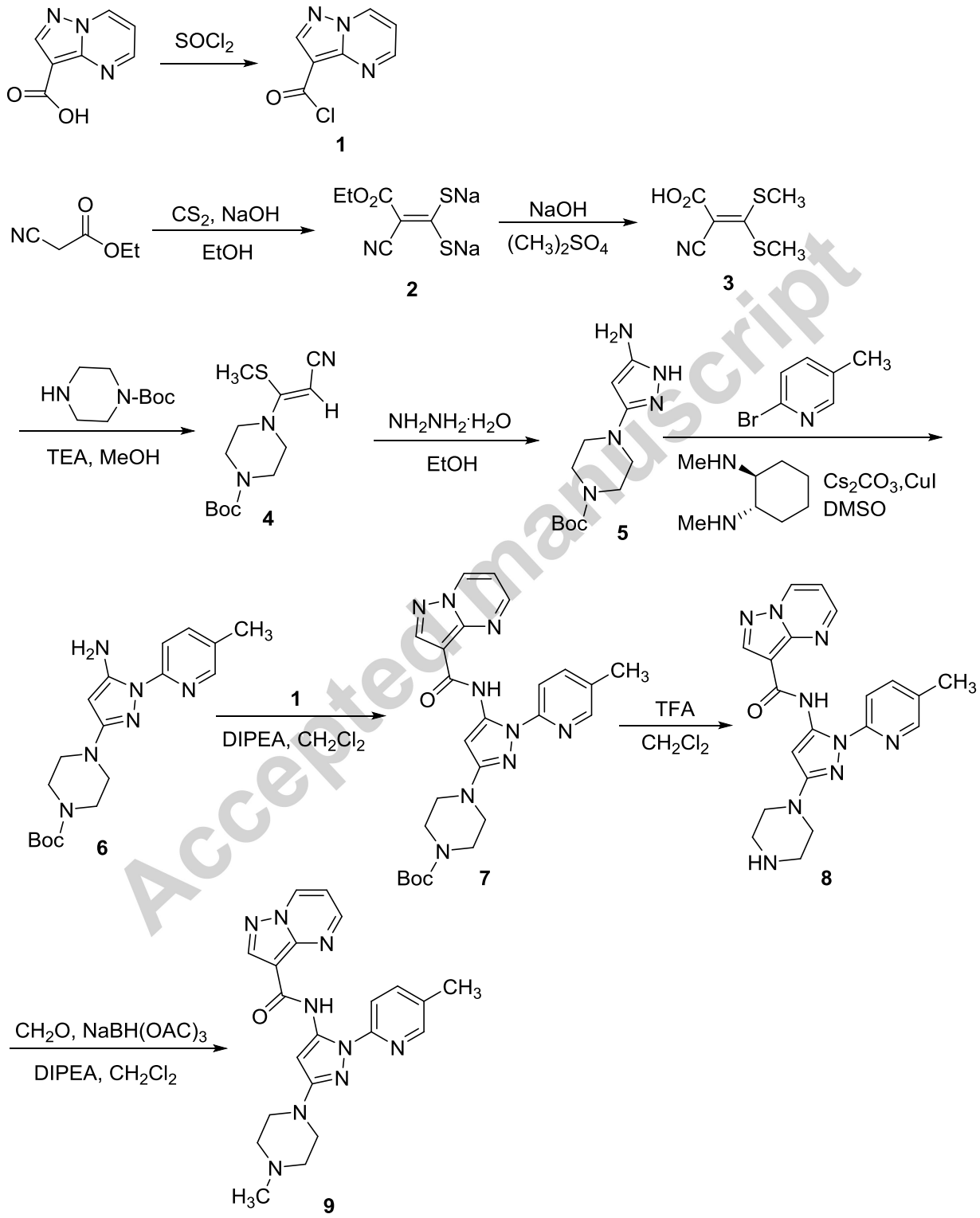

Scheme 2.

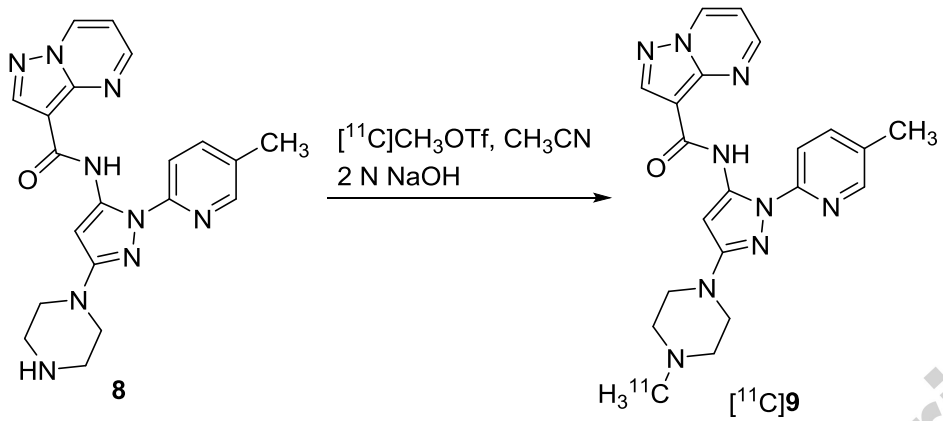

Highlights

- A new carbon-11-labeled amidopyrazole inhibitor of IRAK4 was synthesized.
- A fully automated multi-purpose [^{11}C]-radiosynthesis module was built up.
- A semi-preparative RP HPLC-SPE technique was employed in radiosynthesis.